



# Nasal Dysbiosis in Cutaneous T-Cell Lymphoma Is Characterized by Shifts in Relative Abundances of Non-*Staphylococcus* Bacteria

Madeline J. Hooper<sup>1,7</sup>, Tessa M. LeWitt<sup>1,7</sup>, Francesca L. Veon<sup>1,7</sup>, Yanzhen Pang<sup>1</sup>, George E. Chlipala<sup>2</sup>, Leo Feferman<sup>2</sup>, Stefan J. Green<sup>3</sup>, Dagmar Sweeney<sup>4</sup>, Katherine T. Bagnowski<sup>1</sup>, Michael B. Burns<sup>5</sup>, Patrick C. Seed<sup>6</sup>, Joan Guitart<sup>1</sup> and Xiaolong A. Zhou<sup>1</sup>

The nasal microbiome of patients with cutaneous T-cell lymphoma (CTCL) remains unexplored despite growing evidence connecting nasal bacteria to skin health and disease. Nasal swabs from 45 patients with CTCL (40 with mycosis fungoides, 5 with Sézary syndrome) and 20 healthy controls from the same geographical region (Chicago Metropolitan Area, Chicago, IL) were analyzed using sequencing of 16S ribosomal RNA and *tuf2* gene amplicons. Nasal  $\alpha$ -diversity did not differ between mycosis fungoides/Sézary syndrome and healthy controls (Shannon index, genus level,  $P = 0.201$ ), but distinct microbial communities were identified at the class ( $R^2 = 0.104$ ,  $P = 0.023$ ) and order ( $R^2 = 0.0904$ ,  $P = 0.038$ ) levels. Increased relative abundance of the genera *Catenococcus*, *Vibrio*, *Roseomonas*, *Acinetobacter*, and unclassified Clostridiales was associated with increased skin disease burden ( $P < 0.005$ ,  $q < 0.05$ ). Performed to accurately resolve nasal *Staphylococcus* at the species level, *tuf2* gene amplicon sequencing revealed no significant differences between mycosis fungoides/Sézary syndrome and healthy controls. Although *S. aureus* has been shown to worsen CTCL through its toxins, no increase in the relative abundance of this taxon was observed in nasal samples. Despite the lack of differences in *Staphylococcus*, the CTCL nasal microbiome was characterized by shifts in numerous other bacterial taxa. These data add to our understanding of the greater CTCL microbiome and provide context for comprehending nasal-skin and host-tumor-microbial relationships.

*JID Innovations* (2022);2:100132 doi:10.1016/j.jidinnov.2022.100132

## INTRODUCTION

Cutaneous T-cell lymphoma (CTCL) comprises a heterogeneous group of T-lymphocyte malignancies that infiltrate the skin. Patients with advanced, progressive disease often suffer from profound immune dysregulation and recurrent skin infections. Previous research suggests that the microbiome may influence CTCL pathogenesis, flares, and progression

(Harkins et al., 2021; Lindahl et al., 2019; Willerslev-Olsen et al., 2013). Moreover, distinct microbe-precipitated metabolic and immunologic pathways have been linked to the pathobiology of atopic dermatitis (Nørreslet et al., 2020; Paller et al., 2019), psoriasis (Hidalgo-Cantabrana et al., 2019), hidradenitis suppurativa (McCarthy et al., 2022), and various malignancies (Goodman and Gardner, 2018)—conditions similarly known to be associated with immune dysregulation.

The ecosystem encompassing the nares may be a principal reservoir for self-contamination through nose-to-skin bacterial spread or vice versa. The importance of the nasal microbiome is further emphasized by recent literature suggesting that altered nasal bacterial diversity is associated with gut and skin dysbiosis in hidradenitis suppurativa (McCarthy et al., 2022). Although early culture-based studies have suggested that higher rates of *Staphylococcus aureus* skin and nasal colonization occur in patients with CTCL (Nguyen et al., 2008; Talpur et al., 2008), the complete nasal microbiome in CTCL has yet to be described. Although the CTCL skin microbiota is currently being investigated (Harkins et al., 2021; Salava et al., 2020), its nasal microbial profile is a missing piece of data because CTCL dysbiosis likely extends beyond the skin.

To better understand the CTCL nasal microbiome, we conducted a cross-sectional analysis of the nasal microbiota present in patients with CTCL and healthy controls (HCs)

<sup>1</sup>Department of Dermatology, Northwestern University Feinberg School of Medicine, Chicago, Illinois, USA; <sup>2</sup>Research Informatics Core, Research Resources Center, University of Illinois Chicago, Chicago, Illinois, USA; <sup>3</sup>Rush Genomics and Microbiome Core Facility, Rush University Medical Center, Chicago, Illinois, USA; <sup>4</sup>Genome Research Core, Genome Research Division, Research Resources Center, University of Illinois Chicago, Chicago, Illinois, USA; <sup>5</sup>Department of Biology, Loyola University Chicago, Chicago, Illinois, USA; and <sup>6</sup>Division of Pediatric Infectious Diseases, Ann & Robert H. Lurie Children's Hospital of Chicago, Chicago, Illinois, USA

<sup>7</sup>These authors contributed equally to this work.

Correspondence: Xiaolong A. Zhou, Department of Dermatology, Northwestern University Feinberg School of Medicine, 676 North Street Clair Street, Suite 1600, Chicago, Illinois 60611, USA. E-mail: alan.zhou@northwestern.edu

Abbreviations: CTCL, cutaneous T-cell lymphoma; HC, healthy control; MF, mycosis fungoides; mSWAT, modified Severity Weight Assessment Tool; rRNA, ribosomal RNA; SS, Sézary syndrome

Received 23 January 2022; revised 6 April 2022; accepted 8 April 2022; accepted manuscript published online 28 April 2022; corrected proof published online 16 August 2022

Cite this article as: *JID Innovations* 2022;2:100132

using 16S ribosomal RNA (rRNA) gene sequencing and further determined staphylococcal species relative abundances using *tuf2* gene amplicon sequencing.

## RESULTS

### Patient characteristics

A total of 45 patients comprised the patient group with CTCL, of which 40 had been diagnosed with mycosis fungoïdes (MF), and 5 had been diagnosed with Sézary syndrome (SS) (Table 1 and Supplementary Table S1). All patients and HCs were from the same geographical region (Chicago Metropolitan Area, Chicago, IL) to control for environmental influences on the microbiome (Rothschild et al., 2018). Four HC–CTCL pairs sharing a home were selected for even closer matching. To avoid bias in sample collection, manipulation, and analysis, we concurrently enrolled patients and controls rather than rely on publicly available human microbiome data. There was no significant difference in age, sex, race/ethnicity, or phototype between the two groups (Table 1).

A total of 26 patients had the early-stage disease (stages IA–IIA; 57.8%), and 19 had the advanced-stage disease (stages IIB–IVB; 42.2%); stage IB was the most common overall ( $n = 18$ , 40.0%). The median modified Severity-Weight Assessment Tool (mSWAT) score was 22 (range = 3–100). The most common comorbidities reported were dyslipidemia (MF/SS = 53.3%, HCs = 35.0%), hypertension (MF/SS = 44.4%, HCs = 30.0%), and gastroesophageal reflux (MF/SS = 24.4%, HCs = 30.0%). There were no significant differences in comorbidities between the two groups for these three conditions (Fisher's exact test: dyslipidemia  $P = 0.192$ ; hypertension  $P = 0.411$ ; and gastroesophageal reflux  $P = 0.761$ ) or for any other comorbidity.

### Differences in nasal microbiota between patients and controls

The 16S rRNA gene amplicon sequence data identified a total of 720 genera, 285 families, 139 orders, 67 classes, and 28 phyla. Swab, reagent, and PCR controls were negative for any significant contamination. The most abundant phyla in both groups were the three most frequently encountered in the human nares: *Proteobacteria*, *Actinobacteria*, and *Firmicutes*. At the genus level, there was no significant difference in biodiversity between MF/SS and HC samples as assessed by Shannon diversity index ( $P = 0.201$ ) (Figure 1a). Notably,  $\beta$ -diversity revealed a small but globally significant difference in the microbial community structure between patients and controls on the basis of Adonis/permutterational ANOVA ( $R^2 = 0.104$ ,  $P = 0.023$  for class level;  $R^2 = 0.0904$ ,  $P = 0.038$  for order level) (Figure 1b and c). The most abundant genera in both groups were *Corynebacterium* and *Staphylococcus* (Figure 1d).

Specific taxa contributing to the distinct nasal microbiota of patients with MF/SS were then investigated. Several genera were significantly higher in patients than in HCs ( $q < 0.05$ ): *Roseomonas*, *Catenococcus*, *Vibrio*, *Marinobacter*, *Allo-rhizobium-Neorhizobium-Pararhizobium-Rhizobium*, *Acinetobacter*, *Alishewanella*, *Paracoccus*, unclassified Clostridiales and unclassified Clostridiales family XIII, *Ato-pobium*, and *Dietzia* (Table 2 and Figure 2). Meanwhile, *Lachnospiraceae* NK4A136 group was reduced in patient samples ( $q < 0.05$ ). Regression analyses revealed a positive

**Table 1. Characteristics of Patients ( $n = 45$ ) and Healthy Controls ( $n = 20$ )**

Characteristics	Patients	Controls	P-Value
n	45	20	
Sex <sup>1</sup>			0.2797 <sup>2</sup>
Male	29 (64.4)	10 (50.0)	
Female	16 (35.6)	10 (50.0)	
Age (y) <sup>3</sup>	62.7 (17.5–83.4)	54.5 (24.4–79.1)	0.1393 <sup>2</sup>
Race/Ethnicity <sup>1</sup>			0.9041 <sup>2</sup>
Asian	2 (4.4)	3 (15.0)	
Black	5 (11.1)	0 (0.0)	
White	30 (68.9)	15 (75.0)	
White/Hispanic	6 (13.3)	1 (5.0)	
Other/Hispanic	1 (2.2)	1 (5.0)	
Phototype <sup>1</sup>			0.2398 <sup>2</sup>
Light (FST I–III)	45 (100.0)	19 (95.0)	
Dark (FST IV–VI)	0 (0.0)	1 (5.0)	
Comorbidities <sup>1</sup>			
HTN	20 (44.4)	6 (30.0)	0.411 <sup>4</sup>
DLP	24 (53.3)	7 (35.0)	0.192 <sup>4</sup>
GERD	11 (24.4)	6 (30.0)	0.761 <sup>4</sup>
Diagnosis Subtype <sup>1</sup>			
MF	40 (88.9)	—	
SS	5 (11.1)	—	
Clinical stage <sup>1</sup>			
Early (IA–IIA)	26 (57.8)	—	
Advanced (IIB–IVB)	19 (42.2)	—	
Disease duration (y) <sup>3</sup>	3.1 (0.2–30.0)	—	
mSWAT <sup>3</sup>	22 (3–100)	—	

Abbreviations: DLP, dyslipidemia; FST, Fitzpatrick skin phototype; GERD, gastroesophageal reflux; HTN, hypertension; MF, mycosis fungoïdes; mSWAT, modified Severity Weighted Assessment Tool; SS, Sézary syndrome.

<sup>1</sup>Data are presented as n (%).

<sup>2</sup>Data were analyzed with two-tailed t-test.

<sup>3</sup>Data are presented as median (range).

<sup>4</sup>Data were analyzed with Fisher's exact test.

association between the relative abundance of *Catenococcus*, *Vibrio*, *Roseomonas*, unclassified Clostridiales, and *Acinetobacter* genera and increased mSWAT, an indicator of skin disease burden; reduced *Lachnospiraceae* NK4A136 group relative abundance was associated with higher mSWAT scores (Figure 3). One-way ANOVA revealed significant differences in the mean relative abundance of *Alishewanella*, *Allorhizobium-Neorhizobium-Pararhizobium-Rhizobium*, *Marinobacter*, and *Vibrio* between HCs and patients as grouped by low versus high mSWAT and early versus advanced disease (Supplementary Tables S2–5). Sidak test for pairwise comparisons showed that the mean relative abundance of *Vibrio* was significantly different between HCs and patients with low ( $P = 0.034$ ) and high ( $P = 0.004$ ) mSWAT and between HCs and patients with early-stage ( $P = 0.011$ ) and advanced-stage ( $P = 0.007$ ) disease.

Given the known role of *S. aureus* in worsening CTCL through its toxins (Fujii, 2022), we next examined whether the relative abundances of *Staphylococcus* species differed between patients with MF/SS and HCs. We performed targeted sequencing of the bacterial *tuf* gene, which provides accurate species-level resolution of *Staphylococcus*

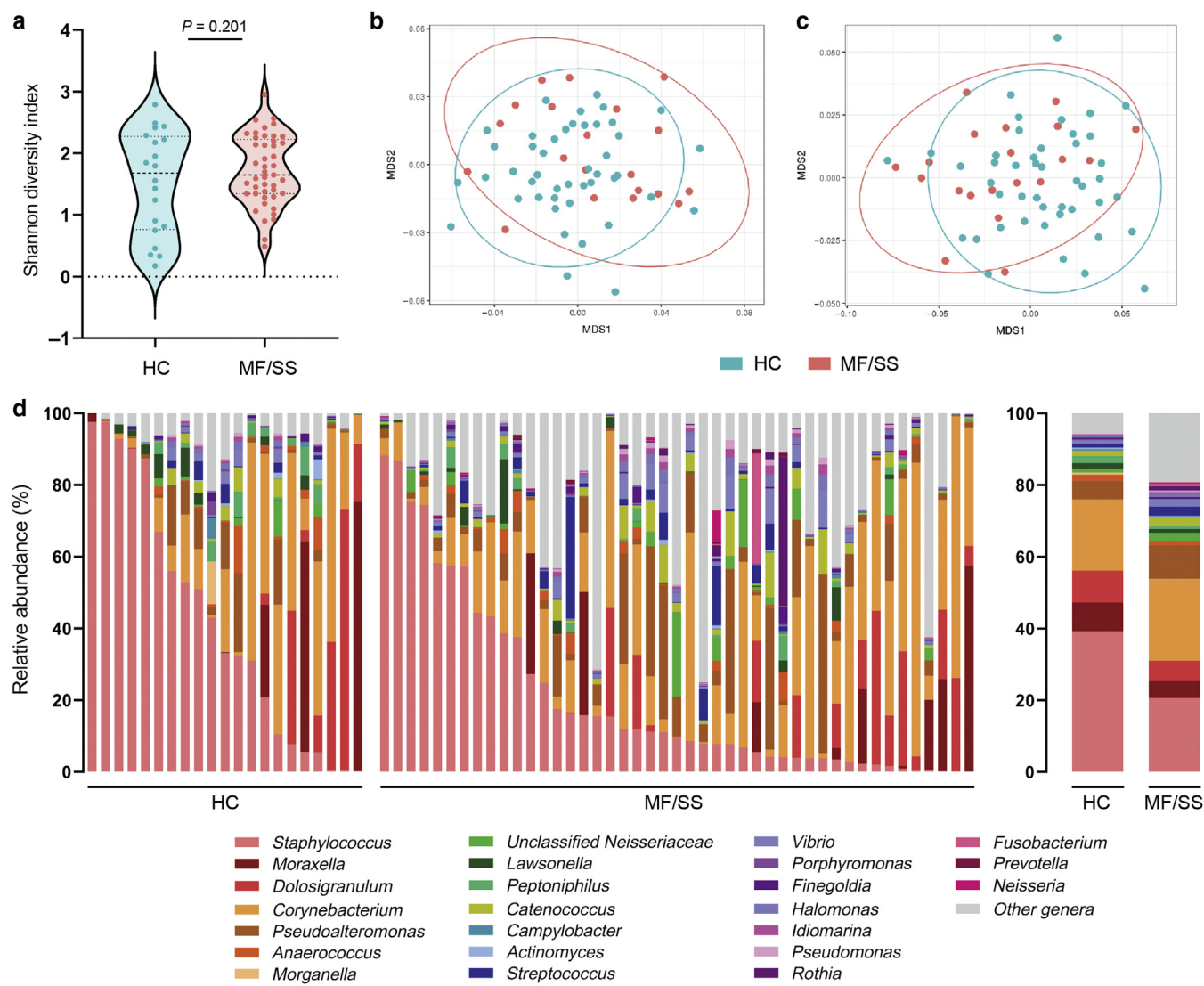


**Figure 1. Distinct nasal bacterial communities were identified in patients with MF/SS versus in HCs.** (a)  $\alpha$ -Diversity was not significantly different between HCs and patients with MF/SS at the genus level (Shannon diversity index,  $P = 0.201$ ). MDS plots using the Bray–Curtis dissimilarity index of  $\beta$ -diversity analyses show significant differential clustering of HCs and patients with MF/SS at the taxonomic levels of (b) class (Adonis/PERMANOVA  $R^2 = 0.104$ ,  $P = 0.023$ ) and (c) order ( $R^2 = 0.0904$ ,  $P = 0.038$ ). (d) Relative abundance (%) of the 20 most abundant genera in nasal samples of HCs and patients with MF/SS (left, individual subjects; right, mean relative abundances per group [HC, MF/SS]). HC, healthy control; MDS, multidimensional scaling; MF, mycosis fungoïdes; PERMANOVA, permutational ANOVA; SS, Sézary syndrome.

communities (Ahle et al., 2021). *S. epidermidis* and *S. aureus* were the most abundant staphylococcal species in both groups: these species comprised 56.8% and 23.8% of all staphylococcal species for patients with MF/SS and 52.7% and 14.5% for HCs, respectively (Supplementary Figure S1). There was no statistically significant difference between the relative abundance of any *Staphylococcus* species (including *S. aureus* and *S. epidermidis*) between patients with MF/SS and HCs (Supplementary Table S6).

## DISCUSSION

Our results show that the nasal microbiomes of patients with MF/SS and HCs are different. These data add to the existing body of knowledge that supports the importance of the nasal microbiome in skin disease (McCarthy et al., 2022; Olesen et al., 2021; Totté et al., 2019). Nasal microbiota are already known to be important in atopic dermatitis, in which

increased relative abundance of nasal *Staphylococcus* and *Moraxella* and decreased *Dolosigranulum* are associated with disease severity (Totté et al., 2019), and increased nasal *S. hominis* is linked to skin *S. hominis* abundance and disease improvement (Olesen et al., 2021). The nares of patients with hidradenitis suppurativa are characterized by enriched *Proteus* communities and reduced *Corynebacterium* (McCarthy et al., 2022). In addition, loss of nasal Proteobacteria has been associated with skin and soft tissue infections (Johnson et al., 2015), and nasal *S. aureus* colonization has been implicated in disease activity in various inflammatory skin conditions, including CTCL (Ng et al., 2017; Nørreslet et al., 2020; Talpur et al., 2008). The nasal microbiome could also feasibly serve as a source for bacterial recolonization of the skin after systemic antibiotic treatment (Lindahl et al., 2021), if not also increase the risk of recurrent infections.

**Table 2. Differential Taxonomic Analysis Shows Unique Microbial Signatures at the Genus Level in Nasal Samples from Patients with MF/SS Versus HCs**

	Genus	HC/Patient LogFC	P-Value	q-Value <sup>1</sup>
Reduced abundance in MF/SS	<i>Lachnospiraceae</i> NK4A136 group	0.51	0.005	0.04
	<i>Ruminococcus</i>	0.12	0.02	0.14
	<i>Ruminoclostridium</i>	0.48	0.03	0.15
Enriched abundance in MF/SS	<i>Catenococcus</i>	-1.41	<0.001	0.001
	<i>Alishewanella</i>	-1.07	<0.001	0.001
	<i>Vibrio</i>	-1.96	<0.001	0.001
	Unclassified Clostridiales family XIII	-0.35	<0.001	0.001
	<i>Roseomonas</i>	-0.89	<0.001	0.001
	Unclassified Clostridiales	-0.62	<0.001	0.001
	<i>Paracoccus</i>	-1.36	<0.001	0.001
	<i>Marinobacter</i>	-1.07	<0.001	0.001
	<i>Atopobium</i>	-0.38	<0.001	<0.005
	<i>Dietzia</i>	-0.62	<0.001	<0.005
<i>Allorhizobium</i> - <i>Neorhizobium</i> - <i>Pararhizobium</i> - <i>Rhizobium</i>	-	-1.32	<0.001	<0.01
	<i>Acinetobacter</i>	-0.99	0.005	0.04
	Unclassified bacteria	-0.59	0.01	0.09
	<i>Christensenellaceae</i> R-7 group	-0.04	0.01	0.09
	<i>Cutibacterium</i>	-0.21	0.02	0.11
	<i>Escherichia/Shigella</i>	-1.04	0.02	0.13
	<i>Neisseria</i>	-0.81	0.03	0.14
	<i>Pseudoalteromonas</i>	-1.7	0.03	0.14
	<i>Subdoligranulum</i>	-0.53	0.04	0.15
	<i>Veillonella</i>	-0.93	0.04	0.17
	<i>Actinomyces</i>	-1.18	0.04	0.17
	Unclassified <i>Gammaproteobacteria</i>	-0.64	0.05	0.17

Abbreviations: FC, fold change; HC, healthy control; MF, mycosis fungoides; SS, Sézary syndrome.

<sup>1</sup>The q-value is the FDR-adjusted P-value (Benjamini and Hochberg, 1995).

Although the exact mechanisms for how the nasal microbiome influences CTCL pathogenesis and vice versa are unclear, the data included in this study provide greater context from which ongoing CTCL skin microbiome research can be understood. We found that enrichment of the genera *Vibrio*, *Roseomonas*, and *Acinetobacter* and depletion of *Paracoccus* are associated with increased skin severity. From the literature, we know that *Vibrio*, *Roseomonas*, and *Acinetobacter* bacteria are important in causing necrotizing fasciitis, aggravating atopic dermatitis, and instigating skin and soft tissue infections, respectively (Table 3 and Supplementary Discussion) (Cerqueira and Peleg, 2011; Janda et al., 1988; Myles et al., 2018); however, their role as nasal bacteria requires further study because there remains an extreme paucity of knowledge on the biological relationships shared by non-*Staphylococcus* species in the nasal microbiome in healthy and disease states.

Importantly, our data showed that the nasal relative abundances of *Staphylococcus* species in patients with CTCL did not differ significantly from those of HCs. Although the pathogenic role of *S. aureus* toxins in CTCL has been well established over the years (Fujii, 2022), it had been unclear whether this translates to a higher relative abundance of *S. aureus* in the skin and/or nose. Previous culture-based studies have either failed to show a statistically significant difference in nasal *S. aureus* colonization rates between patients with CTCL and HCs (Nguyen et al., 2008) or did not include a matched comparison group (Talpur et al., 2008). Our nasal

data, together with recent CTCL skin microbiome data (Harkins et al., 2021), suggest that the effects of *S. aureus* in CTCL may not translate to the actual increased relative abundance of *S. aureus*. Instead, it remains possible that *S. aureus* toxin production—and not relative abundance—differs between patients with CTCL and HCs. These differences between patients and controls may be mediated by shifts in the abundances of the other bacterial taxa. In fact, in atopic dermatitis, quorum sensing between bacterial species in the skin revealed that coagulase-negative staphylococci species produce autoinducing peptides that inhibit *S. aureus* phenol-soluble modulin  $\alpha$ , a proinflammatory virulence factor capable of mediating epidermal injury (Williams et al., 2019).

Nasal dysbiosis carries intriguing insights for pathophysiology in a disease where advanced-stage patients often suffer from recurrent skin infections (Blaizot et al., 2018). Through the accurate characterization of the nasal microbial profiles associated with worse disease, we can conceivably intervene by altering the nasal microbiome through the decolonization of high-risk bacteria or reconstitution with bacteria associated with healthy individuals. The nasal microbiome may have the potential to serve as an additional and accessible biomarker for the determination of disease progression risk. Eventual matched patient skin and nasal microbiome analyses can further elucidate these relationships.

In this study, we establish that CTCL is characterized by nasal dysbiosis composed of shifts in specific non-

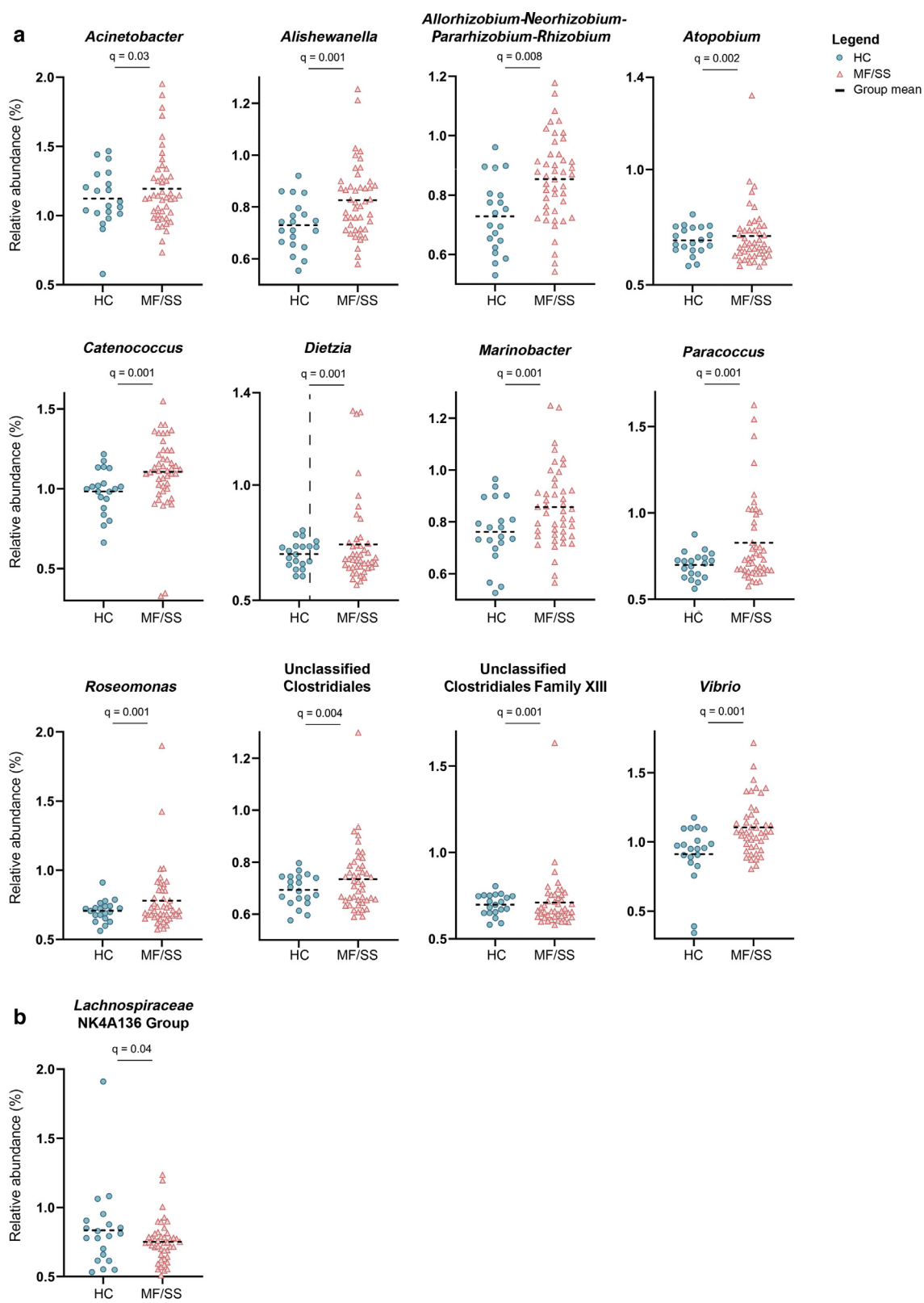
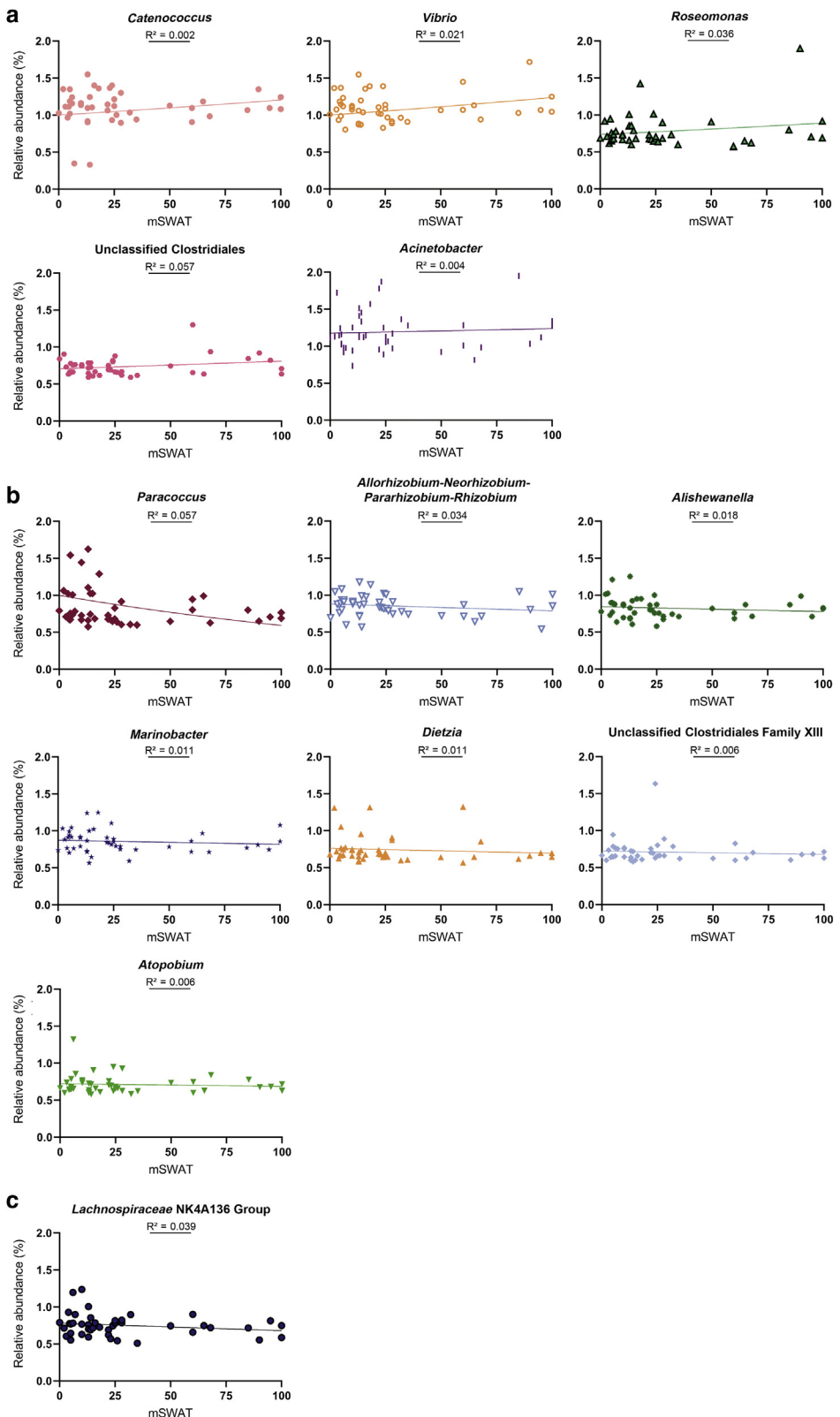


**Figure 2. Changes in the abundance of specific bacterial genera present in the nares of patients with MF/SS compared with those in the nares of the HCs.** Dot plots illustrate the relative sequence abundance (%) of genera that are (a) significantly enriched and (b) significantly reduced in patients with MF/SS versus in HCs. Mean relative abundances are indicated by black horizontal bars. Significance is determined by  $q \leq 0.05$ ; the  $q$ -value is the FDR-adjusted  $P$ -value (Benjamini and Hochberg, 1995). FDR, false discovery rate; HC, healthy control; MF, mycosis fungoides; SS, Sézary syndrome.

**Figure 3. Relationship between the relative abundances of significantly enriched and depleted genera and skin disease burden in patients with MF/SS.** The relative abundance (%) of each genus is plotted versus mSWAT score (an indicator of skin disease burden) with line of best fit. (a) Increased mSWAT score was associated with an increased relative abundance of several genera that were enriched in patients with MF/SS: *Catenococcus*, *Vibrio*, *Roseomonas*, unclassified Clostridiales, and *Acinetobacter*. (b) Lower relative abundances were associated with increased mSWAT scores for the remaining enriched genera: *Paracoccus*, *Allorhizobium-Neorhizobium-Pararhizobium-Rhizobium*, *Alishewanella*, *Marinobacter*, *Dietzia*, unclassified Clostridiales family XIII, and *Atopobium*. (c) Regression analysis of *Lachnospiraceae NK4A136* group (reduced in patients with MF/SS compared with that in the HCs) revealed that lower relative abundances were associated with higher mSWAT scores. HC, healthy control; MF, mycosis fungoïdes; mSWAT, modified Severity-Weight Assessment Tool; SS, Sézary syndrome.



*Staphylococcus* taxa compared with that of healthy individuals. Because bacterial activity perpetuates CTCL disease progression and because infection is the most common cause of death in this patient population (Tsambiras, 2001;

Willerslev-Olsen et al., 2013), attention to the nasal microbiome and its relationship with other microbial reservoirs is crucial to our understanding of the CTCL disease state and pathogenesis.

**Table 3. Summary of Human Disease Associations of Significantly Enriched/Reduced Genera Found in the Anterior Nares of Patients with MF/SS**

Genus	Associations with Human Disease	Associations with Human Cutaneous Disease
<i>Acinetobacter</i>	Hospital- and community-acquired pneumonia, invasive bloodstream infections, urinary tract infections, hospital-acquired meningitis, osteomyelitis, pericarditis	Skin and soft tissue infections
<i>Alishewanella</i>	None available	None available
<i>Allorhizobium</i> - <i>Neorhizobium</i> - <i>Pararhizobium</i> - <i>Rhizobium</i>	None available	None available
<i>Atopobium</i>	Bacteremia, dental infections, bacterial vaginosis	Bacteremia in the setting of Fournier's gangrene
<i>Catenococcus</i>	None available	None available
<i>Dietzia</i>	Bacteremia, prosthetic hip infection, pacemaker infection, pleural fluid isolate	Confluent and reticulated papillomatosis
<i>Lachnospiraceae</i> NK4A136 group	Decreased abundance in the gut microbiome after <i>Trichinella spiralis</i> infection and in patients with dementia; biomarker for lean body habitus	None available
<i>Marinobacter</i>	None available	None available
<i>Paracoccus</i>	<i>P. yeei</i> : myocarditis, peritonitis, bacteremia	None available
<i>Roseomonas</i>	Septicemia <i>R. mucosa</i> : catheter-related infections, dialysis and surgical wound infections, bacteremia	Skin and soft tissue infections, atopic dermatitis
Unclassified Clostridiales	Mediates allergic immune activity	Reduced in the gut microbiome of alopecia areata and pediatric atopic dermatitis
Unclassified Clostridiales family XIII	Mediates mood disorders	None available
<i>Vibrio</i>	Cholera, gastroenteritis, sepsis, less commonly otitis media, meningitis, peritonitis, and pneumonia	Necrotizing fasciitis

Abbreviations: MF, mycosis fungoides; SS, Sézary syndrome.

## MATERIALS AND METHODS

### Participants

Ethical approval was obtained from the Northwestern University Institutional Review Board (STU00209226). Written informed consent, nasal samples, and personal data were obtained at the Northwestern University Cutaneous Lymphoma Clinic (Chicago, Illinois) between 2019 and 2021 in compliance with the Declaration of Helsinki. Each patient had clinically and biopsy-proven CTCL, as reviewed by an expert dermatopathologist (JG). At the time of sample collection, patients were receiving standard-of-care therapies, including skin-directed ( $n = 36$ , 80.0%) and select systemic ( $n = 13$ , 28.9%) treatments or were treatment naive ( $n = 9$ , 18.9%) (Supplementary Table S1). Subjects on any antibiotics within the preceding 4 weeks were excluded. Clinical staging and mSWAT were assessed by the study's principal investigator (XAZ) at sample collection. The HC group ( $n = 20$ ) was composed of age-matched volunteers without CTCL or other skin diseases from the same geographical region.

### Sample collection and DNA extraction

Nasal samples were obtained through sterile swabs (FLOQSwabs, Copan Diagnostics, Murrieta, CA) with hands covered in sterile gloves. All specimens were placed immediately in sterile cryovials and promptly stored at  $-80^{\circ}\text{C}$  until DNA extraction. Genomic DNA was extracted using a Maxwell 16 LEV Blood DNA Kit (Promega, Madison, WI) implemented on a Maxwell 16 Instrument, following the manufacturer's instructions with minor modifications: a lysozyme incubation (10 ng/ $\mu\text{l}$  lysozyme; Thermo Fisher Scientific, Waltham, MA) for 30 minutes at  $37^{\circ}\text{C}$  and bead beating (40 seconds at 6 min/sec) using a FastPrep-24 System (MP Biomedicals, Irvine, CA). Homogenized samples were transferred to the Maxwell cartridges for final DNA purification.

### 16S rRNA gene amplicon sequencing

Genomic DNA was prepared for sequencing using a two-stage amplicon sequencing workflow, as described previously (Naqib et al., 2018), using primers targeting the V4 (fourth hypervariable) region of microbial 16S rRNA genes. The 515 forward modified and 806 reverse modified primers contained 5' linker sequences compatible with access array primers for Illumina sequencers (Fluidigm, South San Francisco, CA) (Walters et al., 2015). PCRs were performed in a total volume of 10  $\mu\text{l}$  using MyTaq HS 2X Mix (Meridian Bioscience, Cincinnati, OH) primers at 500 nM concentration and approximately 1,000 copies per reaction of a synthetic double-stranded DNA template (described below). Extraction blanks and PCR blanks were treated as independent samples and sequenced with unique barcodes. Thermocycling conditions were  $95^{\circ}\text{C}$  for 5 minutes (initial denaturation), followed by 28 cycles of  $95^{\circ}\text{C}$  for 30 seconds,  $55^{\circ}\text{C}$  for 45 seconds, and  $72^{\circ}\text{C}$  for 30 seconds. Second-stage reactions contained 1  $\mu\text{l}$  of PCR product and a unique primer pair of access array primers; thermocycling conditions consisted of  $95^{\circ}\text{C}$  for 5 minutes (initial denaturation), followed by 8 cycles of  $95^{\circ}\text{C}$  for 30 seconds,  $60^{\circ}\text{C}$  for 30 seconds, and  $72^{\circ}\text{C}$  for 30 seconds. Libraries were pooled and sequenced on an Illumina MiniSeq sequencer (Illumina, San Diego, CA) with 15% phiX spike-in and paired-end 2  $\times$  153 base sequencing reads.

A synthetic double-stranded DNA spike-in was synthesized as a gBLOCK by Integrated DNA Technologies (Coralville, IA). The basis of the design was a 999 base pairs region of the 16S rRNA gene of *Rhodanobacter denitrificans* strain 2APBS1T (NC\_020541) (Prakash et al., 2012). Portions of V1, V2, and V4 variable regions were replaced by eukaryotic mRNA sequences (*Apostichopus japonicus Gapdh* mRNA, HQ292612; and *Strongylocentrotus intermedius Gapdh* mRNA, KC775387). Primer sites were preserved, and the

overall length in the base pair of the synthetic DNA did not differ from the equivalent *R. denitrificans* fragment. PCR amplicons generated from this synthetic DNA do not differ in size from bacterial amplicons and can only be identified and removed through postsequencing bioinformatics analysis. The sequence can be accessed through GenBank using the accession number OK324963.

### **tuf2 amplicon next-generation sequencing**

Genomic DNA was PCR amplified with primers ACAGTGACGA-CATGGTTCTACAACAGGCCGTGTTAACGTG for CS1\_tuf2 forward and TACGGTACAGAGACTTGGTCTACAGTACGTCCACCTT CACG for CS2\_tuf2 reverse (Ahle et al., 2021, 2020) targeting the *Staphylococcus tuf* gene. Amplicons were generated using a two-stage PCR amplification protocol as previously described (Naqib et al., 2018). First-stage PCR amplifications were performed in 10 µl reactions in 96-well plates using MyTaq HS 2X mastermix (Meridian Bioscience). PCR conditions were 95°C for 5 minutes, followed by 28 cycles of 95°C for 30 seconds, 55°C for 30 seconds, and 72°C for 60 seconds. Second-stage reactions using access array primers were performed as described earlier. Samples were pooled, purified, and sequenced on an Illumina MiSeq with 10% phiX spike-in and paired-end 2 × 300 base sequencing reads (i.e., V3 chemistry). Library preparation, pooling, and sequencing were performed at the Genome Research Core within the Research Resources Center at the University of Illinois Chicago (Chicago, IL).

### **Sequence data processing (DADA2)**

To check for contamination, control swab, PCR, and reagent/kit samples were performed. In total, 22 PCR and 32 extraction controls were analyzed, all of which yielded very low sequence counts (mean ± SD: 122.5 ± 61.4), far below the 5,000 counts per sample threshold needed for inclusion in data analyses.

16S rRNA gene amplicon reads were merged using PEAR, version 0.9.6 (Zhang et al., 2014), and trimmed using cutadapt, version 1.18, to remove ambiguous nucleotides and primer sequences on the basis of a quality threshold of  $P = 0.01$  (Martin, 2011). Reads lacking the primer sequence and/or sequences <225 base pairs after merging and quality trimming were discarded. Chimeric sequences were identified and removed using the USEARCH algorithm with a comparison with Silva (version 132) reference sequence (Edgar, 2010; Glöckner et al., 2017). Amplicon sequence variants were identified using DADA2, version 1.18 (Callahan et al., 2016), and annotated taxonomically using the Naive Bayesian classifier included in DADA2 with the Silva (version 132) training set. Synthetic spike-in sequences were removed before proceeding with downstream bioinformatics analyses. Diversity analyses were performed in R using the vegan library, version 2.5-6 (Okansen et al., 2018). Biodiversity ( $\alpha$ -diversity) was calculated using the Shannon index modeled with the sample covariates using a generalized linear model assuming Gaussian distribution. Bray–Curtis indices were calculated to assess sample dissimilarity ( $\beta$ -diversity).

For the *tuf2* next-generation sequencing, merged reads that lacked either primer sequence or were <400 base pairs were discarded. Chimeric sequences were identified and removed in a de novo fashion using USEARCH, version 8.1.1861 (Edgar, 2010). Amplicon sequence variants were identified using the protocol described earlier and taxonomically annotated using alignment from BLAST (blastn) with the RefSeq Prokaryotic Genomes reference, downloaded on 1 December 2021 (NCBI Resource Coordinators, 2017).

### **Differential analysis of microbial taxa**

Differential analyses of taxa as compared with experimental covariates were performed using edgeR (version 3.28.1) on raw sequence counts (McCarthy et al., 2012). The 16S data were filtered to remove sequences of chloroplast, mitochondrial, or eukaryotic origin and taxa present in <30% of all samples and with <500 total sequence counts across all samples. The *tuf2* next-generation sequencing data were filtered to retain only species belonging to the genus *Staphylococcus* and to remove taxa following the same parameters as mentioned earlier. Data were normalized as counts per million and fit using a negative binomial generalized linear model using experimental covariates.

### **Statistical analyses**

Statistical analyses were performed in R and STATA SE. Significance of the  $\alpha$ -diversity model (ANOVA) was tested using the F-test. Posthoc, pairwise analyses were performed using the Mann–Whitney test (Wickham, 2009). The dissimilarity indices were tested for significance using Adonis/permutational ANOVA, and additional comparisons of the individual covariates were performed using analysis of similarities. Statistical tests for the differential analyses were performed using a likelihood ratio test. Adjusted  $P$ -values (q-values) were calculated using the Benjamini–Hochberg false discovery rate correction (Benjamini and Hochberg, 1995). Significant taxa were determined on the basis of a false discovery rate threshold of 5.0% (0.05). Plots were generated using GraphPad Prism, version 9.2, (GraphPad Software, San Diego, CA) and the ggplot2 library in R (Wickham, 2009).

### **Data availability statement**

Datasets related to this article can be found at <https://dataview.ncbi.nlm.nih.gov/object/PRJNA768111?reviewer=pd94ec0d6iurp8k0gbs5evtjhj> (National Center for Biotechnology Information Short Read Archive, accession number PRJNA768111).

### **ORCIDs**

Madelaine J. Hooper: <http://orcid.org/0000-0003-1334-5342>  
Tessa M. LeWitt: <http://orcid.org/0000-0001-8935-2165>  
Francesca L. Veon: <http://orcid.org/0000-0002-0232-1671>  
Yanzhen Pang: <http://orcid.org/0000-0003-1825-9603>  
George E. Chlipala: <http://orcid.org/0000-0003-0203-3191>  
Leo Feferman: <http://orcid.org/0000-0002-5821-3434>  
Stefan J. Green: <http://orcid.org/0000-0003-2781-359X>  
Dagmar Sweeney: <http://orcid.org/0000-0001-6320-8931>  
Katherine T. Bagnowski: <http://orcid.org/0000-0002-7482-4454>  
Michael B. Burns: <http://orcid.org/0000-0001-9791-4359>  
Patrick C. Seed: <http://orcid.org/0000-0001-8998-8374>  
Joan Guitart: <http://orcid.org/0000-0001-7635-9237>  
Xiaolong A. Zhou: <http://orcid.org/0000-0002-6177-2472>

### **AUTHOR CONTRIBUTIONS**

Conceptualization: XAZ, TML, FLV, MJH, JG; Data Curation: XAZ, TML, YP, KTB; Formal Analysis: GEC, LF, SJG, XAZ; Funding Acquisition: XAZ; Investigation: XAZ, TML, FLV, MJH, YP, KTB, DS; Methodology: GEC, LF, SJG; Project Administration: XAZ, JG; Resources: XAZ, KTB, JG, DS, SJG; Software: GEC, LF; Supervision: XAZ, PCS, JG; Validation: XAZ, MBB, GEC; Visualization: GEC, LF, XAZ, FLV; Writing - Original Draft Preparation: TML, FLV, MJH, XAZ; Writing - Review and Editing: XAZ, JG, MBB, SJG, GEC, FLV, MJH, TML

### **CONFLICT OF INTEREST**

The authors state no conflict of interest.

### **ACKNOWLEDGMENTS**

The authors would like to thank the patients who contributed to the study. XAZ is supported in part by a career development award from the Dermatology Foundation, a Cutaneous Lymphoma Foundation Catalyst Research

Grant, and an institutional grant from Northwestern University Clinical and Translational Sciences Institute and the National Institutes of Health (grant number 5KL2TR001424).

## SUPPLEMENTARY MATERIAL

Supplementary material is linked to the online version of the paper at [www.jidonline.org](http://www.jidonline.org), and at <https://doi.org/10.1016/j.jid.2022.100132>.

## REFERENCES

- Ahle CM, Stødkilde K, Afshar M, Poehlein A, Ogilvie LA, Söderquist B, et al. *Staphylococcus saccharolyticus*: an overlooked human skin colonizer. *Microorganisms* 2020;8:1105.
- Ahle CM, Stødkilde-Jørgensen K, Poehlein A, Streit WR, Hüpeden J, Brüggemann H. Comparison of three amplicon sequencing approaches to determine staphylococcal populations on human skin. *BMC Microbiol* 2021;21:221.
- Benjamini Y, Hochberg Y. Controlling the false discovery rate: a practical and powerful approach to multiple testing. *J R Stat Soc Series B Stat Methodol* 1995;57:289–300.
- Blairoz R, Ouattara E, Fauconneau A, Beylot-Barry M, Pham-Ledard A. Infectious events and associated risk factors in mycosis fungoïdes/Sézary syndrome: a retrospective cohort study. *Br J Dermatol* 2018;179:1322–8.
- Callahan BJ, McMurdie PJ, Rosen MJ, Han AW, Johnson AJA, Holmes SP. DADA2: high-resolution sample inference from Illumina amplicon data. *Nat Methods* 2016;13:581–3.
- Cerdeira GM, Peleg AY. Insights into *Acinetobacter baumannii* pathogenicity. *IUBMB Life* 2011;63:1055–60.
- Edgar RC. Quality measures for protein alignment benchmarks. *Nucleic Acids Res* 2010;38:2145–53.
- Fujii K. Pathogenesis of cutaneous T cell lymphoma: involvement of *Staphylococcus aureus*. *J Dermatol* 2022;49:202–9.
- Glöckner FO, Yilmaz P, Quast C, Gerken J, Beccati A, Ciuprina A, et al. 25 years of serving the community with ribosomal RNA gene reference databases and tools. *J Biotechnol* 2017;261:169–76.
- Goodman B, Gardner H. The microbiome and cancer. *J Pathol* 2018;244:667–76.
- Harkins CP, MacGibeny MA, Thompson K, Bubic B, Huang X, Brown I, et al. Cutaneous T-cell lymphoma skin microbiome is characterized by shifts in certain commensal bacteria but not viruses when compared with healthy controls. *J Invest Dermatol* 2021;141:1604–8.
- Hidalgo-Cantabrana C, Gómez J, Delgado S, Requena-López S, Queiroz-Silva R, Margolles A, et al. Gut microbiota dysbiosis in a cohort of patients with psoriasis. *Br J Dermatol* 2019;181:1287–95.
- Janda JM, Powers C, Bryant RG, Abbott SL. Current perspectives on the epidemiology and pathogenesis of clinically significant *Vibrio* spp. *Clin Microbiol Rev* 1988;1:245–67.
- Johnson RC, Ellis MW, Lanier JB, Schlett CD, Cui T, Merrell DS. Correlation between nasal microbiome composition and remote purulent skin and soft tissue infections. *Infect Immun* 2015;83:802–11.
- Lindahl LM, Iversen L, Ødum N, Kilian M. *Staphylococcus aureus* and antibiotics in cutaneous T-cell lymphoma. *Dermatology* 2021;1–3.
- Lindahl LM, Willemslev-Olsen A, Gjerdum LMR, Nielsen PR, Blümel E, Rittig AH, et al. Antibiotics inhibit tumor and disease activity in cutaneous T-cell lymphoma. *Blood* 2019;134:1072–83.
- McCarthy DJ, Chen Y, Smyth GK. Differential expression analysis of multi-factor RNA-Seq experiments with respect to biological variation. *Nucleic Acids Res* 2012;40:4288–97.
- McCarthy S, Barrett M, Kirthi S, Vlckova K, Tobin AM, Murphy M, et al. Altered skin and gut microbiome in hidradenitis suppurativa. *J Invest Dermatol* 2022;142:459–68.e15.
- Martin M. Cutadapt removes adapter sequences from high-throughput sequencing reads. *EMBnetjournal* 2011;17:10–2.
- Myles IA, Earland NJ, Anderson ED, Moore IN, Kieh MD, Williams KW, et al. First-in-human topical microbiome transplantation with Roseomonas mucosa for atopic dermatitis. *JCI Insight* 2018;3:e120608.
- Naqib A, Poggi S, Wang W, Hyde M, Kunstman K, Green SJ. Making and sequencing heavily multiplexed, high-throughput 16S ribosomal RNA gene amplicon libraries using a flexible, two-stage PCR protocol. *Methods Mol Biol* 2018;1783:149–69.
- NCBI Resource Coordinators. Database resources of the National Center for Biotechnology Information. *Nucleic Acids Res* 2017;45:D12–7.
- Ng CY, Huang YH, Chu CF, Wu TC, Liu SH. Risks for *Staphylococcus aureus* colonization in patients with psoriasis: a systematic review and meta-analysis. *Br J Dermatol* 2017;177:967–77.
- Nguyen V, Huggins RH, Lertsburapa T, Bauer K, Rademaker A, Gerami P, et al. Cutaneous T-cell lymphoma and *Staphylococcus aureus* colonization. *J Am Acad Dermatol* 2008;59:949–52.
- Nørreslet LB, Edslev SM, Andersen PS, Plum F, Holt J, Kjerulf A, et al. Colonization with *Staphylococcus aureus* in patients with hand eczema: prevalence and association with severity, atopic dermatitis, subtype and nasal colonization. *Contact Dermatitis* 2020;83:442–9.
- Okansen J, Blanchet FG, Kindt R, Legendre P, Minchin P, O'Hara R, et al. Vegan: community ecology package. R package version 2018;2:4–6.
- Olesen CM, Ingham AC, Thomsen SF, Clausen ML, Andersen PS, Edslev SM, et al. Changes in skin and nasal microbiome and staphylococcal species following treatment of atopic dermatitis with dupilumab. *Microorganisms* 2021;9:1487.
- Paller AS, Kong HH, Seed P, Naik S, Scharschmidt TC, Gallo RL, et al. The microbiome in patients with atopic dermatitis [published correction appears in *J Allergy Clin Immunol* 2019;143:1660]. *J Allergy Clin Immunol* 2019;143:26–35.
- Prakash O, Green S, Jasrotia P, Overholt W, Canion A, Watson DB, et al. Description of *Rhodanobacter denitrificans* sp. nov., isolated from nitrate-rich zones of a contaminated aquifer. *Int J Syst Evol Microbiol* 2012;62:2457–62.
- Rothschild D, Weissbrod O, Barkan E, Kurilshikov A, Korem T, Zeevi D, et al. Environment dominates over host genetics in shaping human gut microbiota. *Nature* 2018;555:210–5.
- Salava A, Deptula P, Lyyski A, Laine P, Paulin L, Väkevä L, et al. Skin microbiome in cutaneous T-cell lymphoma by 16S and whole-genome shotgun sequencing. *J Invest Dermatol* 2020;140:2304–8.e7.
- Talpur R, Bassett R, Duvic M. Prevalence and treatment of *Staphylococcus aureus* colonization in patients with mycosis fungoïdes and Sézary syndrome. *Br J Dermatol* 2008;159:105–12.
- Totté JEE, Pardo LM, Fieten KB, Vos MC, Broek TJ, Schuren FHJ, et al. Nasal and skin microbiomes are associated with disease severity in paediatric atopic dermatitis. *Br J Dermatol* 2019;181:796–804.
- Tsambiras PE, Patel S, Greene JN, Sandin RL, Vincent AL. Infectious complications of cutaneous T-cell lymphoma. *Cancer Control* 2001;8:185–8.
- Walters W, Hyde ER, Berg-Lyons D, Ackermann G, Humphrey G, Parada A, et al. Improved bacterial 16S rRNA gene (V4 and V4-5) and fungal internal transcribed spacer marker gene primers for microbial community surveys. *mSystems* 2015;1:e00009–15.
- Wickham H. ggplot2: Elegant graphics for data analysis. New York: Springer New York; 2009.
- Willemslev-Olsen A, Krejsgaard T, Lindahl LM, Bonefeld CM, Wasik MA, Koralov SB, et al. Bacterial toxins fuel disease progression in cutaneous T-cell lymphoma. *Toxins (Basel)* 2013;5:1402–21.
- Williams MR, Costa SK, Zaramela LS, Khalil S, Todd DA, Winter HL, et al. Quorum sensing between bacterial species on the skin protects against epidermal injury in atopic dermatitis. *Sci Transl Med* 2019;11:eaat8329.
- Zhang J, Kobert K, Flouri T, Stamatakis A. PEAR: a fast and accurate Illumina Paired-End reAd mergeR. *Bioinformatics* 2014;30:614–20.



This work is licensed under a Creative Commons Attribution-NonCommercial-NoDerivatives 4.0 International License. To view a copy of this license, visit <http://creativecommons.org/licenses/by-nc-nd/4.0/>

## SUPPLEMENTARY MATERIALS AND DISCUSSION

### **Acinetobacter**

The genus *Acinetobacter* comprises a complex and heterogeneous group of Gram-negative, strictly aerobic coccobacilli (Visca et al., 2011). *Acinetobacter* is an emergent pathogen that can cause life-threatening infections (Cerdeira and Peleg, 2011). Owing to its extensive virulence and profound resistance to currently available antibiotics, this genus is responsible for substantial morbidity and mortality among critically ill patients in both hospital and community settings (Visca et al., 2011). Notably, the species *A. baumannii* has been described as the Gram-negative equivalent to methicillin-resistant *Staphylococcus aureus* (Visca et al., 2011). In addition to bloodstream infections, *A. baumannii* causes ventilator-associated and community-acquired pneumonia—the most frequent clinical manifestations of *Acinetobacter* infection (Cerdeira and Peleg, 2011; Munoz-Price and Weinstein, 2008). Of note, higher rates of morbidity are attributed to *Acinetobacter*-related pneumonia versus to any other species (Wisplinghoff et al., 2012). Recently, a rare case of purulent endocarditis caused by carbapenem-resistant *A. baumannii* was reported (Liu et al., 2019). Other clinically relevant *Acinetobacter* species include *A. pittii* and *A. nosocomialis*, which commonly cause urinary tract infections, hospital-acquired meningitis, traumatic skin and soft tissue infections, and osteomyelitis (Cerdeira and Peleg, 2011).

### **Alishewanella**

*Alishewanella* is a genus of Gram-negative, facultatively anaerobic bacteria with four known species, of which only one has been identified within human tissue (Vogel et al., 2000); however, this genus has yet to be linked to human disease.

### **Allorhizobium-Neorhizobium-Pararhizobium-Rhizobium**

*Allorhizobium-Neorhizobium-Pararhizobium-Rhizobium* is a genus of Gram-negative bacteria found in soil. This genus has yet to be linked to human disease.

### **Atopobium**

The genus *Atopobium* represents anaerobic, Gram-positive bacteria commensal to the vagina and oral mucosa (Angelakis et al., 2009; Dauby et al., 2019). *A. vaginalis* is a common cause of bacterial vaginosis, but it has also been associated with intrapartum bacteremia (Dauby et al., 2019). Typically found in the gingiva, *A. rimate* and *A. parvulum* are known to precipitate chronic periodontitis, and more rarely, cases of *A. rimate* bacteremia have been reported (Angelakis et al., 2009; Devresse et al., 2016). Two cases of *Atopobium*-related sepsis have occurred in patients with Fournier's gangrene, thus indicating that these species may contribute to the pathogenesis of this fulminant form of necrotizing fasciitis (Cools et al., 2014; Oyaert et al., 2014). Furthermore, studies of the lung microbiota in sarcoidosis and cystic fibrosis have suggested that *Atopobium* is a disease-associated bacterial genus (Surette, 2014; Zimmermann et al., 2017).

### **Catenococcus**

The *Catenococcus* genus represents a group of Gram-negative, facultatively anaerobic bacteria with only one known species, *C. thiocyclus*. This genus has yet to be linked to human disease.

### **Dietzia**

Members of the *Dietzia* genus are Gram-positive, aerobic, environmental actinomycetes (Koerner et al., 2009). Three *Dietzia* species are known to be pathogenic to humans. *D. maris* has been implicated in bacteremia and infectious aortitis in immunocompromised patients, as well as prosthetic hip and pacemaker infections in immunocompetent individuals (Bemer-Melchior et al., 1999; Perkin et al., 2012; Pidoux et al., 2001; Reyes et al., 2006). One case of pleural *D. cinnamomea* isolated from a patient with stage IV mesothelioma has been published, but the patient was asymptomatic (Cawcett et al., 2016). Finally, *D. pappillomatosis* was identified within skin scrapings from a patient with confluent and reticular papillomatosis, also known as Gougerot-Carteaud syndrome, a benign and rare skin disorder thought to have a bacterial etiology given its response to antibiotics (Jones et al., 2008).

### **Lachnospiraceae NK4A136 group**

A short-chain fatty acid (SCFA) producer, the *Lachnospiraceae* NK4A136 group has been identified as an anti-inflammatory, probiotic bacterium with potent beneficial effects as a member of the gut microbiome (Stadlbauer et al., 2020). Recent research on the gut microbiota in individuals with obesity versus in lean individuals showed that this bacterium is negatively associated with body fat and is significantly depleted in obese groups, thus suggesting that *Lachnospiraceae* NK4A136 group may be a biomarker for

lean habitus in humans (Companys et al., 2021). Reduced levels of *Lachnospiraceae* NK4A136 group in the gut have also been identified in patients with dementia and after *Trichinella spiralis* infection (Chen et al., 2021; Stadlbauer et al., 2020).

### **Marinobacter**

*Marinobacter* is a genus of Gram-negative bacteria commonly found in seawater. This genus has yet to be linked to human disease.

### **Paracoccus**

A total of 17 soil- and brine-based species are categorized within the genus *Paracoccus*, but only *P. yeei* has been associated with human infections. A study of *P. yeei* revealed that its unique virulence is due to the acquisition of specific, pathoadaptive genomic sequences (Lasek et al., 2018). Still, infections with this species are rare and only known to occur in immunocompromised individuals (Fosso et al., 2021). Case reports involving *P. yeei* consist of myocarditis in a transplanted heart, peritonitis in peritoneal dialysis, and bacteremia in the setting of cirrhosis (Fosso et al., 2021).

### **Roseomonas**

*Roseomonas* represents an opportunistic group of pink-pigmented, Gram-negative coccobacilli that is typically associated with septicemia, followed by urogenital and soft tissue infections in patients with underlying immunocompromising conditions (Struthers et al., 1996). The species *R. mucosa* and *R. gilardii* have been identified as virulent and highly infectious microbes (Struthers et al., 1996). *R. mucosa* has been cited in catheter, dialysis, and surgery-related infections (Romano-Bertrand et al., 2016), and a rare case of infective endocarditis bacteremia caused by *R. mucosa* in a patient with systemic lupus erythematosus has been described (Shao et al., 2019). Moreover, research suggests that opportunistic infections caused by *R. mucosa* are due to patient skin microbiota rather than the environment (Romano-Bertrand et al., 2016). *Roseomonas* infections have been associated with various coexisting diseases such as peritonitis, abscess formation, bacteremia, community-acquired secondary bacterial infections, and infectious spondylitis (Shao et al., 2019).

A recent study of the role of Gram-negative skin bacteria in atopic dermatitis (AD) revealed that application of *R. mucosa* isolates collected from healthy volunteers improved outcomes in mouse and cell culture models of AD, whereas application of AD-sourced *R. mucosa* had either no impact on or worsened outcomes in the same models (Myles et al., 2018). Treatment of AD with topical *R. mucosa* obtained from healthy volunteers was associated with significant decreases in measures of AD severity, topical steroid requirements, and *S. aureus* burden (Myles et al., 2018). These preclinical results suggest that interventions targeting the microbiome could provide therapeutic benefits for patients with AD.

### **Unclassified Clostridiales and unclassified Clostridiales family XIII**

The class Clostridia encompasses a group of SCFA producers that are commensal to the human gut, including unclassified Clostridiales and unclassified Clostridiales family XIII. Largely considered beneficial to human health, Clostridia can modulate immune activity and allergic reactions through interactions with colonic regulatory T cells (Furusawa et al., 2013). SCFAs are also considered anti-inflammatory; depleted levels of the order Clostridiales have been observed in the guts of patients with alopecia areata, and the loss of anti-inflammatory SCFAs is postulated to bridge this microbial alteration and autoimmune skin disease (Moreno-Arribes et al., 2020). In this same study about the gut microbiome in alopecia areata, Clostridiales family XIII was significantly more abundant in controls (Moreno-Arribes et al., 2020). Loss of gut Clostridia has also been associated with increased eosinophilia and earlier age of onset in pediatric AD (Lee et al., 2016). Finally, an investigation of the microbial influence on mood disorders showed that serum Clostridiales family XIII DNA levels are positively correlated with anxiety symptoms, but the gut microbiota of patients with anxiety is characterized by decreased Clostridiales family XIII abundance compared with that of the controls (Rhee et al., 2021). As a growing area of study, it is hypothesized that reduced gut Clostridiales mediates psychiatric diseases through the gut-brain axis and downstream effects of abnormal intestinal amino acid metabolism and SCFA formation (Li et al., 2020).

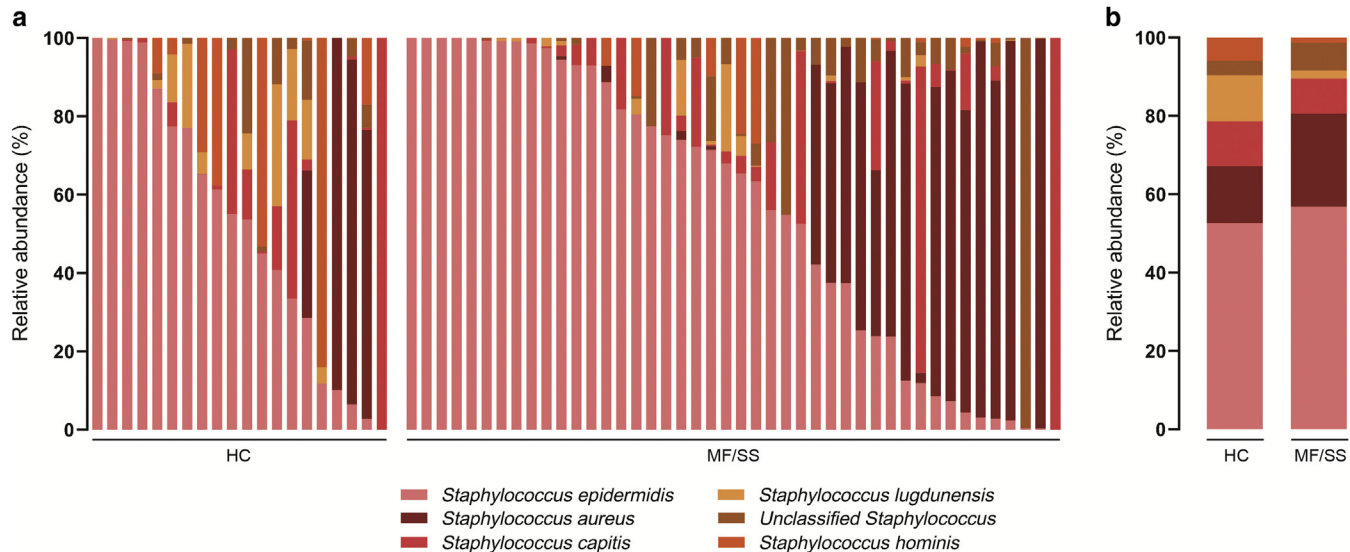
### **Vibrio**

Vibriosis represents a general term for a group of clinical conditions of varying severity associated with the genus *Vibrio*, whose members are facultatively anaerobic, Gram-negative bacilli. The three most common *Vibrio* species involved in human illness in the United States include *V. parahaemolyticus*, *V. vulnificus*, and *V. alginolyticus*. Infections range from mild gastroenteritis to septicemia or invasive skin and soft tissue infections. Less common, *Vibrio*

is responsible for cases of otitis media, meningitis, peritonitis, and pneumonia. Life-threatening *Vibrio* infections include cholera and necrotizing fasciitis (Janda et al., 1988). Miscellaneous *Vibrio* species have been isolated from numerous anatomic sites, including the ear, eye, gallbladder, sinuses, peritoneal fluid, and urine; these account for <5% of all noncholera infections. The chief risk factors for *Vibrio* infection include the consumption of raw, undercooked seafood or shellfish and trauma associated with a marine environment. Less than 15% of all *Vibrio* species have been associated with human disease, whereas the remaining taxa are solely environmental (Janda et al., 1988).

#### SUPPLEMENTARY REFERENCES

- Angelakis E, Roux V, Raoult D, Drancourt M. Human case of *Atopobium rimae* bacteremia. *Emerg Infect Dis* 2009;15:354–5.
- Bemer-Melchior P, Haloun A, Riegel P, Drugeon HB. Bacteremia due to *Dietzia maris* in an immunocompromised patient. *Clin Infect Dis* 1999;29:1338–40.
- Benjamini Y, Hochberg Y. Controlling the false discovery rate: a practical and powerful approach to multiple testing. *J R Stat Soc Series B Stat Methodol* 1995;57:289–300.
- Cawcett KA, Bhatti MM, Nelson DR. Pleural fluid infection caused by *Dietzia cinnamea*. *Diagn Microbiol Infect Dis* 2016;85:496–7.
- Cerdeira GM, Peleg AY. Insights into *Acinetobacter baumannii* pathogenicity. *IUBMB Life* 2011;63:1055–60.
- Chen HL, Xing X, Zhang B, Huang HB, Shi CW, Yang GL, et al. Higher mucosal type II immunity is associated with increased gut microbiota diversity in BALB/c mice after *Trichinella spiralis* infection. *Mol Immunol* 2021;138:87–98.
- Companys J, Gosalbes MJ, Pla-Pagà L, Calderón-Pérez L, Llauradó E, Pedret A, et al. Gut microbiota profile and its association with clinical variables and dietary intake in overweight/obese and lean subjects: a cross-sectional study. *Nutrients* 2021;13:2032.
- Cools P, Oyaert M, Vaneechoutte M, De Laere E, Vervaeke S. *Atopobium deltae* sp. nov., isolated from the blood of a patient with Fournier's gangrene. *Int J Syst Evol Microbiol* 2014;64:3140–5.
- Dauby N, Martiny D, Busson L, Cogan A, Meghraoui A, Argudín MA, et al. *Atopobium vaginae* intrapartum bacteremia: a case report with a literature review. *Aerobe* 2019;59:212–4.
- Devresse A, Labriola L, Dossin T, Vatlet M, Hantson P. *Atopobium rimae* bacteremia complicated by an infection-related glomerulonephritis in a cardiac transplanted patient. *Transpl Infect Dis* 2016;18:637–8.
- Fosso C, Maillart E, Beun B, Touzani F, Mahadeb B, Clevenbergh P. Opportunistic peritonitis in peritoneal dialysis: the example of *Paracoccus yeei*. *Clin Case Rep* 2021;9:e04176.
- Furusawa Y, Obata Y, Fukuda S, Endo TA, Nakato G, Takahashi D, et al. Commensal microbe-derived butyrate induces the differentiation of colonic regulatory T cells [published correction appears in *Nature* 2014;506:254]. *Nature* 2013;504:446–50.
- Janda JM, Powers C, Bryant RG, Abbott SL. Current perspectives on the epidemiology and pathogenesis of clinically significant *Vibrio* spp. *Clin Microbiol Rev* 1988;1:245–67.
- Jones AL, Koerner RJ, Natarajan S, Perry JD, Goodfellow M. *Dietzia papillomatosis* sp. nov., a novel actinomycete isolated from the skin of an immunocompetent patient with confluent and reticular papillomatosis. *Int J Syst Evol Microbiol* 2008;58:68–72.
- Koerner RJ, Goodfellow M, Jones AL. The genus *Dietzia*: a new home for some known and emerging opportunist pathogens. *FEMS Immunology & Medical Microbiology* 2009;55(3):296–305.
- Lasek R, Szuplewska M, Mitura M, Decewicz P, Chmielowska C, Pawłot A, et al. Genome Structure of the Opportunistic Pathogen *Paracoccus yeei* (Alphaproteobacteria) and Identification of Putative Virulence Factors. *Front Microbiol* 2018;9:2553.
- Lee EMDP, Lee S-YMDP, Kang M-JP, Kim KBS, Won SP, Kim B-JMDP, et al. Clostridia in the gut and onset of atopic dermatitis via eosinophilic inflammation. *Ann Allergy Asthma Immunol* 2016;117:91–2, e1.
- Li J, Ma Y, Bao Z, Gui X, Li AN, Yang Z, et al. Clostridiales are predominant microbes that mediate psychiatric disorders. *Journal of Psychiatric Research* 2020;130:48–56.
- Liu J, Xiao X, Cen C, Yuan H, Yang M. Rare purulent pericarditis caused by carbapenem-resistant *Acinetobacter baumannii*: a case report. *Medicine (Baltimore)* 2019;98:e17034.
- Moreno-Arrores OM, Serrano-Villar S, Perez-Brocá V, Saceda-Corralo D, Morales-Raya C, Rodrigues-Barata R, et al. Analysis of the gut microbiota in alopecia areata: identification of bacterial biomarkers. *J Eur Acad Dermatol Venereol* 2020;34:400–5.
- Munoz-Price LS, Weinstein RA. *Acinetobacter* infection. *N Engl J Med* 2008;358:1271–81.
- Myles IA, Earland NJ, Anderson ED, Moore IN, Kieh MD, Williams KW, et al. First-in-human topical microbiome transplantation with *Roseomonas mucosa* for atopic dermatitis. *JCI Insight* 2018;3:e120608.
- Oyaert M, Cools P, Breyne J, Heyvaert G, Vandewiele A, Vaneechoutte M, et al. Sepsis with an *Atopobium*-like species in a patient with Fournier's gangrene. *J Clin Microbiol* 2014;52:364–6.
- Perkin S, Wilson A, Walker D, McWilliams E. *Dietzia* species pacemaker pocket infection: an unusual organism in human infections. *BMJ Case Rep* 2012;2012:bcr1020115011.
- Pidoux O, Argenson JN, Jacomo V, Drancourt M. Molecular identification of a *Dietzia maris* hip prosthesis infection isolate. *J Clin Microbiol* 2001;39:2634–6.
- Reyes G, Navarro JL, Gamallo C, delas Cuevas MC. Type A aortic dissection associated with *Dietzia maris*. *Interact Cardiovasc Thorac Surg* 2006;5:666–8.
- Rhee SJ, Kim H, Lee Y, Lee HJ, Park CHK, Yang J, et al. The association between serum microbial DNA composition and symptoms of depression and anxiety in mood disorders. *Sci Rep* 2021;11:13987.
- Romano-Bertrand S, Bourdier A, Aujoulat F, Michon AL, Masnou A, Parer S, et al. Skin microbiota is the main reservoir of *Roseomonas mucosa*, an emerging opportunistic pathogen so far assumed to be environmental. *Clin Microbiol Infect* 2016;22:737.e1–7.
- Shao S, Guo X, Guo P, Cui Y, Chen Y. *Roseomonas mucosa* infective endocarditis in patient with systemic lupus erythematosus: case report and review of literature. *BMC Infect Dis* 2019;19:140.
- Stadlbauer V, Engertsberger L, Komarova I, Feldbacher N, Leber B, Pichler G, et al. Dysbiosis, gut barrier dysfunction and inflammation in dementia: a pilot study. *BMC Geriatr* 2020;20:248.
- Struthers M, Wong J, Janda JM. An initial appraisal of the clinical significance of *Roseomonas* species associated with human infections. *Clin Infect Dis* 1996;23:729–33.
- Surette MG. The cystic fibrosis lung microbiome. *Ann Am Thorac Soc* 2014;11(Suppl 1):S61–5.
- Visca P, Seifert H, Towner KJ. *Acinetobacter* infection – an emerging threat to human health. *IUBMB Life* 2011;63:1048–54.
- Vogel BF, Venkateswaran K, Christensen H, Falsen E, Christiansen G, Gram L. Polyphasic taxonomic approach in the description of *Alishewanella fetalis* gen. nov., sp. nov., isolated from a human foetus. *Int J Syst Evol Microbiol* 2000;50:1133–42.
- Wisplinghoff H, Paulus T, Lugenheim M, Stefanik D, Higgins PG, Edmond MB, et al. Nosocomial bloodstream infections due to *Acinetobacter baumannii*, *Acinetobacter pittii* and *Acinetobacter nosocomialis* in the United States. *J Infect* 2012;64:282–90.
- Zimmermann A, Knecht H, Häslер R, Zissel G, Gaede KI, Hofmann S, et al. *Atopobium* and *Fusobacterium* as novel candidates for sarcoidosis-associated microbiota. *Eur Respir J* 2017;50:1600746.



**Supplementary Figure S1. Relative abundance of staphylococcal species in patients with MF/SS compared with those in HCs.** (a) Relative abundance (%) of *Staphylococcus* species present in the nasal samples of HCs and patients by individual subjects. (b) Mean relative abundances (%) per study group. HC, healthy control; MF, mycosis fungoïdes; SS, Sézary syndrome.

**Supplementary Table S1. Detailed Demographic Characteristics of Patients with MF/SS (n = 45) and Healthy Controls (n = 20)**

Gender	Age (y)	Race/Ethnicity	Diagnosis	Stage	mSWAT	Comorbidities	Skin-Directed Therapy	Systemic Therapy
Healthy controls (n = 20)								
F	34	Asian	—	—	—	None	—	—
M	25	Asian	—	—	—	None	—	—
M	26	White	—	—	—	None	—	—
M	37	White	—	—	—	None	—	—
M	24	Asian	—	—	—	None	—	—
F	27	White/ Hispanic	—	—	—	None	—	—
F	60	White	—	—	—	GERD, DLP, hypothyroidism, migraines, rheumatoid arthritis	—	—
F	68	White	—	—	—	DLP	—	—
M	76	White	—	—	—	GERD, DLP, HTN, T2DM	—	—
F	74	White	—	—	—	Asthma, CM, CKD (stage III), GERD, DLP, HTN, hypothyroidism, T2DM	—	—
F	54	White	—	—	—	None	—	—
M	55	White	—	—	—	None	—	—
F	65	White	—	—	—	GERD, DLP, T2DM	—	—
F	74	White	—	—	—	GERD, DLP, HTN	—	—
M	38	Other/ Hispanic	—	—	—	GERD, HTN	—	—
M	79	White	—	—	—	HTN	—	—
F	54	White	—	—	—	None	—	—
F	58	White	—	—	—	DLP, HTN, hypothyroidism, T2DM	—	—
M	66	White	—	—	—	None	—	—
M	47	White	—	—	—	None	—	—
Patient with MF/SS (n = 45)								
M	71	White	FMF	IIIB	35	Bladder cancer, GERD, DLP, T2DM	TCS	Acitretin
M	65	White	FMF	IIIA	90	GERD	TCS	—
F	18	White/ Hispanic	FMF	IB	26	Asthma, GERD	TCS, NBUVB	IFN- $\alpha$ -2b
M	56	White/ Hispanic	FMF	IB	16	Anemia, CKD, GERD, glaucoma, DLP, HTN, T2DM, vertebral osteomyelitis	TCS, TCI, NBUVB	—
F	72	White	FMF	IB	5	Diverticulitis, GERD, DLP, hypothyroidism, infiltrating ductal carcinoma	TCS	IFN- $\alpha$ -2b, bexarotene
M	36	White/ Hispanic	FMF	IB	3	DLP, T2DM	TCS	—
F	74	White	FMF	IIB	18	DLP, HTN	TCS, TCI	Acitretin

(continued)

Supplementary Table S1. Continued

Gender	Age (y)	Race/Ethnicity	Diagnosis	Stage	mSWAT	Comorbidities	Skin-Directed Therapy	Systemic Therapy
F	35	Other/Hispanic	FMF	IB	28	None	—	—
F	63	Black	FMF	IIB	13	DLP, HTN, hypothyroidism, obesity	TCS, NBUVB	—
M	67	White	FMF/SMF	IB	13	DLP, HTN	TCS, NBUVB, XRT	IFN- $\alpha$ -2b, acitretin
M	55	White	FMF/SMF	IB	3	None	TCS, NBUVB	—
M	69	White	CD4+ MF	IIB	7	CAD, insomnia, obesity, overactive bladder	TCS	—
M	49	Asian	CD4+ MF	IB	60	Cataracts, ED, mitral regurgitation, obesity, T2DM	—	—
M	37	White/Hispanic	CD4+ MF	IIB	65	None	TCS, NBUVB	IFN- $\alpha$ -2b
M	47	White	CD4+ MF	IB	4	GERD, obesity	TCS	—
M	58	White	CD4+ MF	IIA	22	Autoimmune hemolytic anemia, anaplastic large cell lymphoma, asthma, HTN, hyperthyroidism, obesity, OSA	TCS	Acitretin
M	65	White	CD4+ MF	IA	13	GERD, HTN, DLP, OSA, T2DM	TCS	—
F	37	White/Hispanic	CD4+ MF	IB	25	HTN, hypothyroidism, OSA	TCS, NBUVB	Bexarotene, acitretin
F	72	Black	CD4+ MF	IIIA	100	DLP, HTN, T2DM	TCS	—
M	69	White	CD4+ MF	IIIA	14	AF, BPH, CAD, DLP, T2DM	TCS	—
M	67	White	CD4+ MF	IIB	4.5	CRC, DLP	TCS, Imiquimod	Acitretin
M	52	White	CD4+ MF	IB	13	Allergic rhinitis	TCS	—
M	81	White	CD4+ MF	IB	10	BPH, DLP, PAF, prostate cancer	TCS	Bexarotene
F	74	White	CD4+ MF	IA	5	Hypothyroidism	TCS	—
M	65	White	CD4+ MF	IA	5	DLP, GERD, HTN, obesity, T2DM	TCS	—
M	61	White	CD4+ MF	IA	6	HTN	TCS	—
F	26	White	CD4+ MF	IB	68	Migraine	—	—
M	63	White	CD4+ MF	IIB	6	Hypothyroidism	TCS	—
F	72	Black	CD4+ MF	IIIA	85	Glaucoma, DLP, HTN	TCS	—
F	61	White	CD4+ MF	IA	2	GERD, endometriosis, osteoporosis, primary hyperparathyroidism	—	—
M	74	White	CD4+ MF	IA	22	Osteoarthritis, BPH, CKD, GERD, glaucoma, HTN, ulnar neuropathy	TCS	Methotrexate, bexarotene
M	46	Black	CD4+ MF	IIB	60	Asthma, bronchitis	TCS	—
M	62	White	CD4+ MF	IB	23	DLP	—	—
F	55	White	CD4+ MF	IB	25	Asthma, COPD, GERD, DLP, HTN, PAD, PFO	—	—
M	68	White	CD4+ MF	IIB	50	DLP, HTN	—	—
M	55	White	CD4+ MF	IB	10	DLP, HTN, obesity	—	—

(continued)

**Supplementary Table S1. Continued**

Gender	Age (y)	Race/Ethnicity	Diagnosis	Stage	mSWAT	Comorbidities	Skin-Directed Therapy	Systemic Therapy
M	72	White	CD4+ MF	IIIB	95	Atrial flutter, anxiety, cervical stenosis, CKD, ED, DLP, HTN, lumbar disc herniation, OSA, PAF, prostate cancer, tachycardia-induced CM	TCS	Brentuximab vedotin
F	58	Asian	CD4+ MF	IB	14	Breast cancer, DLP, HTN, multinodular goiter, T2DM	TCS	—
M	29	White/ Hispanic	CD8+ MF	IB	24	None	TCS	—
F	46	White	CD8+ MF	IA	15	Allergic rhinitis, fibroids, obesity	—	—
M	66	White	SS	IV	10	AF, dysphagia, DLBCL, DLP, HSV keratitis, hypothyroidism	TCS	—
F	56	White	SS	IV	24	DLP, HTN, hypothyroidism	TCS	—
M	83	White	SS	IV	100	CAD, HTN	TCS	Methotrexate
F	66	White	SS	IV	28	DLP, hypothyroidism	TCS	—
M	67	Black	SS	IV	32	Atrial flutter, CAD, ED, HFrEF, DLP, HTN, obesity, T2DM	TCS	—

Abbreviations: AF, atrial fibrillation; BPH, benign prostatic hyperplasia; CAD, coronary artery disease; CM, cardiomyopathy; CKD, chronic kidney disease; COPD, chronic obstructive pulmonary disease; CRC, colorectal carcinoma; DLBCL, diffuse large B-cell lymphoma; DLP, dyslipidemia; ED, erectile dysfunction; F, female; FMF, folliculotropic mycosis fungoides; GERD, gastroesophageal reflux disease; HFrEF, heart failure with reduced ejection fraction; HSV, herpes simplex virus; HTN, hypertension; LCT, large cell transformation; M, male; MF, mycosis fungoides; mSWAT, modified Severity Weighted Assessment Tool; NBUVB, narrowband UVB; OSA, obstructive sleep apnea; PAD, peripheral artery disease; PAF, paroxysmal atrial fibrillation; PFO, patent foramen ovale; SMF, syringotropic mycosis fungoides; SS, Sézary syndrome; T2DM, type 2 diabetes mellitus; TCI, topical calcineurin inhibitor; TCS, topical corticosteroids; XRT, localized radiotherapy.

**Supplementary Table S2. Mean Relative Abundances (%) of Genera Identified on Differential Analysis Comparing Bacterial Communities in the Samples of HCs Versus in Patients with MF/SS—One-Way ANOVA: HCs Versus MF/SS, Organized by mSWAT Score**

Genus	HCs	Patients with MF/SS		P-Value
		mSWAT < 10	mSWAT ≥ 10	
<i>Acinetobacter</i>	1.123	1.132	1.213	0.386
<i>Alishewanella</i>	0.729	0.884	0.807	0.006
<i>Allorhizobium-Neorhizobium-Pararhizobium-Rhizobium</i>	0.729	0.869	0.850	0.005
<i>Atopobium</i>	0.693	0.748	0.700	0.405
<i>Catenococcus</i>	0.984	1.079	1.115	0.087
<i>Dietzia</i>	0.701	0.788	0.727	0.329
<i>Lachnospiraceae NK4A136 group</i>	0.835	0.786	0.740	0.269
<i>Marinobacter</i>	0.761	0.882	0.849	0.042
<i>Paracoccus</i>	0.699	0.887	0.807	0.054
<i>Roseomonas</i>	0.707	0.742	0.792	0.303
Unclassified Clostridiales	0.693	0.731	0.736	0.378
Unclassified Clostridiales family XIII	0.698	0.713	0.708	0.950
<i>Vibrio</i>	0.912	1.111	1.104	0.003

Abbreviations: HC, healthy control; MF, mycosis fungoides; mSWAT, modified Severity Weighted Assessment Tool; SS, Sézary syndrome.

**Supplementary Table S3. Mean Relative Abundances (%) of Genera Identified on Differential Analysis Comparing Bacterial Communities in the Samples of HCs Versus in Patients with MF/SS—Sidak Method for Pairwise Comparisons: HCs Versus MF/SS, Organized by mSWAT Score**

Group 1	Group 2	Mean Difference	P-Value
<i>Alishewanella</i>			
HC	MF/SS, mSWAT < 10	0.155	0.005
HC	MF/SS, mSWAT ≥ 10	0.078	0.096
MF/SS, mSWAT < 10	MF/SS, mSWAT ≥ 10	-0.077	0.232
<i>Allorhizobium-Neorhizobium-Pararhizobium-Rhizobium</i>			
HC	MF/SS, mSWAT < 10	0.140	0.028
HC	MF/SS, mSWAT ≥ 10	0.121	0.009
MF/SS, mSWAT < 10	MF/SS, mSWAT ≥ 10	-0.019	0.971
<i>Marinobacter</i>			
HC	MF/SS, mSWAT < 10	0.120	0.082
HC	MF/SS, mSWAT ≥ 10	0.088	0.095
MF/SS, mSWAT < 10	MF/SS, mSWAT ≥ 10	-0.03	0.885
<i>Vibrio</i>			
HC	MF/SS, mSWAT < 10	0.200	0.034
HC	MF/SS, mSWAT ≥ 10	0.192	0.004
MF/SS, mSWAT < 10	MF/SS, mSWAT ≥ 10	-0.008	0.999

Abbreviations: HC, healthy control; MF, mycosis fungoides; mSWAT, modified Severity Weighted Assessment Tool; SS, Sézary syndrome.

**Supplementary Table S4. Mean Relative Abundances (%) of Genera Identified on Differential Analysis Comparing Bacterial Communities in the Samples of HCs Versus in Patients with MF/SS—One-Way ANOVA: HC Versus MF/SS, Organized by Clinical Stage**

Genus	Patients with MF/SS			<i>P</i> -Value
	HC	I A–IIA	IIB–IVB	
<i>Acinetobacter</i>	1.123	1.181	1.210	0.551
<i>Alishewanella</i>	0.729	0.843	0.803	0.016
<i>Allorhizobium-Neorhizobium-Pararhizobium-Rhizobium</i>	0.729	0.881	0.818	0.002
<i>Atopobium</i>	0.693	0.692	0.739	0.332
<i>Catenococcus</i>	0.984	1.157	1.036	0.015
<i>Dietzia</i>	0.701	0.736	0.750	0.600
<i>Lachnospiraceae NK4A136 group</i>	0.835	0.707	0.813	0.077
<i>Marinobacter</i>	0.761	0.868	0.842	0.044
<i>Paracoccus</i>	0.699	0.858	0.784	0.049
<i>Roseomonas</i>	0.707	0.714	0.869	0.011
Unclassified Clostridiales	0.693	0.720	0.755	0.220
Unclassified Clostridiales family XIII	0.698	0.739	0.669	0.242
<i>Vibrio</i>	0.912	1.096	1.119	0.003

Abbreviations: HC, healthy control; MF, mycosis fungoides; SS, Sézary syndrome.

**Supplementary Table S5. Mean Relative Abundances (%) of Genera Identified on Differential Analysis Comparing Bacterial Communities in the Samples of HCs Versus in Patients with MF/SS—Sidak Method for Pairwise Comparisons: HC Versus MF/SS, Organized by Clinical Stage**

Group 1	Group 2	Mean Difference	<i>P</i> -Value
<i>Alishewanella</i>			
HC	MF/SS, I A–IIA	0.114	0.013
HC	MF/SS, IIB–IVB	0.074	0.220
MF/SS, I A–IIB	MF/SS, IIB–IVB	-0.040	0.663
<i>Allorhizobium-Neorhizobium-Pararhizobium-Rhizobium</i>			
HC	MF/SS, I A–IIA	0.152	0.001
HC	MF/SS, IIB–IVB	0.089	0.130
MF/SS, I A–IIB	MF/SS, IIB–IVB	-0.063	0.350
<i>Catenococcus</i>			
HC	MF/SS, I A–IIA	0.173	0.016
HC	MF/SS, IIB–IVB	0.053	0.800
MF/SS, I A–IIB	MF/SS, IIB–IVB	-0.120	0.148
<i>Marinobacter</i>			
HC	MF/SS, I A–IIA	0.106	0.044
HC	MF/SS, IIB–IVB	0.081	0.225
MF/SS, I A–IIB	MF/SS, IIB–IVB	-0.026	0.912
<i>Paracoccus</i>			
HC	MF/SS, I A–IIA	0.159	0.043
HC	MF/SS, IIB–IVB	0.085	0.512
MF/SS, I A–IIB	MF/SS, IIB–IVB	-0.744	0.581
<i>Roseomonas</i>			
HC	MF/SS, I A–IIA	0.159	0.043
HC	MF/SS, IIB–IVB	0.085	0.512
MF/SS, I A–IIB	MF/SS, IIB–IVB	-0.744	0.581
<i>Vibrio</i>			
HC	MF/SS, I A–IIA	0.184	0.011
HC	MF/SS, IIB–IVB	0.207	0.007
MF/SS, I A–IIB	MF/SS, IIB–IVB	0.024	0.974

Abbreviations: HC, healthy control; MF, mycosis fungoides; SS, Sézary syndrome.

**Supplementary Table S6. Differential Analysis for *Staphylococcus* Species Reveals No Statistically Significant Differences between the Nasal Microbiota of Patients with MF/SS and HCs**

	<i>Staphylococcus</i> Species	Patient/HC LogFC	P-Value	q-Value <sup>1</sup>
Reduced abundance in MF/SS	<i>S. lugdunensis</i>	-2.54	0.14	0.43
	<i>S. hominis</i>	-1.92	0.16	0.43
	<i>S. capitis</i>	-0.29	0.73	0.82
Enriched abundance in MF/SS	Unclassified <i>Staphylococcus</i>	1.48	0.22	0.43
	<i>S. aureus</i>	0.72	0.82	0.82
	<i>S. epidermidis</i>	0.19	0.74	0.82

Abbreviations: FC, fold change; FDR, false discovery rate; HC, healthy control; MF, mycosis fungoides; SS, Sézary syndrome.

<sup>1</sup>The q-value is the FDR-adjusted P-value (Benjamini and Hochberg, 1995).